

Scientific paper

Stochastic Approach to Shrinkage Cracking Control for Reinforced Concrete Structural Elements

Tetsushi Kanda¹, Haruki Momose¹, Kei-ichi Imamoto² and Hirozo Mihashi³

Received 22 June 2007, accepted 5 December 2007

Abstract

This study aims at evaluating shrinkage cracking risk in reinforced concrete structures, which has not been established in the past studies. To achieve this goal, analytical scheme capable of calculating the probability of shrinkage cracking was proposed. In this scheme, the variation of shrinkage restrained stress, that of concrete cracking strength, and safety factor are to be determined. The first two were determined with simple analytical simulation of structural elements, and the last factor was based on the comparison between cracking record of actual RC member and analysis results. Finally, this scheme was applied to actual construction project, and its validity was confirmed during the construction process.

1. Introduction

With an increase in building stock, technology of controlling shrinkage cracking, which greatly affects the durability of reinforced concrete (R/C) buildings, has significant potential for making a social contribution. However, despite the fact that it has been a major subject of research over the years, the efforts to establish a shrinkage crack control technology have been confined to empirical inquiries, and any systematic solution has yet to be proposed (AIJ 2002).

Although many studies on elemental technologies of elucidating or controlling the shrinkage cracking resulted in a very rich accumulation of findings (AIJ 2003a), no research has ever integrated the elemental technologies to a design of controlling the shrinkage cracking. Regarding the prediction of crack initiation that forms an important part of the control technology, very few research have been successful in predicting cracking taking into account driving and resisting factors and their impacts in a quantitative manner. As an example of relevant past studies, Li *et al.* (2006) proposed a procedure to assess cracking risks in bridge deck elements. They quantitatively evaluated cracking risks in the elements by employing finite element numerical simulation and showed effects of concrete mix selection such as involvement of shrinkage reducing agents. However, their results are restricted in simulating cracking tendency in the elements and not compared with actual structures' behavior. Furthermore, van Breugel and Lockhorst (2001) suggested clear calculation procedure to estimate early age cracking risk adopting stochastic ap-

proach. However, their results are limited only for early age hardening concrete tested in laboratory and involve no comparison with field data in actual structures. Hence results in available literature appear insufficient to construct comprehensive design scheme capable of controlling shrinkage cracking in a practical manner.

On this basis, the present study proposes a shrinkage crack control technique capable of assessing the risk of shrinkage cracking and verifies the accuracy of the proposed technique focusing on planar elements restrained by beams. First, adopting the probability of shrinkage cracking P_f as an index of shrinkage cracking risk, a basic model is presented to calculate P_f based on the stress-strength ratio η , which is defined by the ratio of shrinkage restraint stress σ_{st} to cracking strength σ_{cr} . Next, estimation equations are derived in terms of explicit functions for σ_{st} and σ_{cr} for planar elements. To calculate P_f based on the basic model, three values are needed, the dispersion of σ_{st} and σ_{cr} and the safety factor. They are determined through analysis, as well as based on the crack data of each element. Finally, the proposed technique is applied to cracking control in an actual construction project to verify its effectiveness and accuracy.

2. Basic model for cracking probability calculation

The S-R (Stress-Resistance) model, commonly applied to structural safety evaluation (e.g., Ang and Tang 1984, Tokumaru *et al.* 1987), is adopted in this study. It is also used to obtain the probability of cracking induced by autogenous shrinkage and cement hydration heat (JSCE 2002a, van Breugel and Lockhorst 2001). When applying the S-R model to the problem of shrinkage cracking, it is assumed that cracking occurs when the crack-driving force S , i.e. the shrinkage restraint stress, exceeds the critical level of resistance force R , i.e. the shrinkage cracking strength, ($R \leq S$). The cracking probability is calculated on the assumption that S and R are random variables that follow a certain probability distribution. Thus, the crack-

¹Building Construction and Materials Group, Kajima Technical Research Institute, Tokyo, Japan.

E-mail: kandat@kajima.com

²Department of Architecture, Ashikaga Institute of Technology, Ashikaga, Japan.

³Department of Architecture and Building Science, Tohoku University, Sendai, Japan.

ing probability P_f is given by (Nakamura *et al.* 1999):

$$P_f = \text{Prob}(Z=R-S \leq 0) \quad (1)$$

Assuming R and S are independent from each other and follow normal distributions, the calculation of P_f is significantly simplified, as in (Imamoto *et al.* 2004):

$$P_f = \Phi\left[\frac{(\xi-1)}{\sqrt{\text{COV}[R]^2 + \xi^2 \cdot \text{COV}[S]^2}}\right] \quad (2)$$

where, Φ : standard normal probability distribution function; $\text{COV}[S]$ and $\text{COV}[R]$: coefficient of variation for S and R , respectively; $\xi = \eta \cdot \gamma$; η : stress-strength ratio ($= \sigma_{st} / \sigma_{cr} = (\mu_S / \mu_R) / \gamma$); μ_S and μ_R : expected values of S and R , respectively; γ : safety factor; σ_{st} : estimate of shrinkage restraint stress (N/mm²); σ_{cr} : estimate of shrinkage cracking strength (N/mm²). Denotation γ here represents a correction factor to compensate for an error produced when estimating S and R by means of σ_{st} and σ_{cr} , respectively.

Using Equation (2) and determining the three set values, i.e., $\text{COV}[S]$, $\text{COV}[R]$ and γ will derive a unique solution of P_f as a function of η (hereinafter called the ‘‘shrinkage crack risk curve’’). Denotation η is expressed as the ratio of σ_{st} to σ_{cr} , and if these two values are estimated based on the properties of R/C elements, it becomes possible to evaluate the cracking risk of the elements. This evaluation provides us with necessary engineering solutions to control shrinkage cracking in design of R/C elements. In the following chapters, a technique calculating σ_{st} and σ_{cr} and determining $\text{COV}[R]$, $\text{COV}[S]$ and γ will be discussed.

3. Method of calculating shrinkage restraint stress and cracking strength

3.1 Principle of establishing equations for shrinkage restraint stress and cracking strength

With walls and floor slabs, this study examines σ_{st} induced in planar elements restrained by beams at a low drying shrinkage rate, as well as σ_{cr} when cracks occur in the elements. In literature, sophisticated numerical analysis methods can reproduce σ_{st} induced in planer elements and their accuracy has also been examined already (e.g., Bolander and Berton 2004, Kwak and Ha 2006). However, they usually require complicated calculation procedure and thus are not completely suitable for application to the general-purpose design of actual structures. With regard to the latter, i.e., cracking strength, the results vary by literatures, and no definite findings have been obtained (JCI 2001).

Hence, this study aims at establishing a control design technique based on the stochastic theory and derives equations that have the following characteristics:

- The equations should be as simple as possible to be put into practice of R/C design and construction.
- Considering that they are utilized to estimate $\text{COV}[S]$ and $\text{COV}[R]$, σ_{st} and σ_{cr} should be expressed as explicit functions.

3.2 Shrinkage restraint stress equations using the effective Young's modulus

The effective Young's modulus method (Iwaki *et al.* 1980) has the characteristics described above and is adopted to derive estimation equations for the shrinkage restraint stress of planar elements externally restrained by beams. The basic stress-strain equations using the effective Young's modulus method are given by (Iwaki *et al.* 1980, Imamoto 2003).

$$\sigma(t_{i+1/2}) = \sum_{j=1}^i E_e(t_{i+1/2}, t_j) \Delta \varepsilon_e(t_j) \quad (3)$$

$$E_e(t_{i+1/2}, t_j) = \frac{E_c(t_j)}{1 + \{E_c(t_j) / E_{28}\} \phi(t_{i+1/2}, t_j)} \quad (4)$$

$$\Delta \varepsilon_e(t_j) = \Delta \varepsilon(t_j) - \Delta \varepsilon_f(t_j) \quad (5)$$

where,

$\sigma(t_{i+1/2})$: stress in concrete at Step $t_{i+1/2}$ (N/mm²),

$E_e(t_{i+1/2}, t_j)$: effective Young's modulus (N/mm²),

$\phi(t_{i+1/2}, t_j)$: creep coefficient at Step $t_{i+1/2}$ when loaded at Step t_j ,

(Ratio of creep strain to elastic strain assuming Young's modulus at 28-day age),

$\Delta \varepsilon(t_j)$: increment of response strain at Step t_j ,

$\Delta \varepsilon_f(t_j)$: increment of free strain at Step t_j ,

$\Delta \varepsilon_e(t_j)$: increment of restraint strain at Step t_j ,

$E_c(t_j)$: Young's modulus at Step t_j (N/mm²),

E_{28} : Young's modulus under standard curing at 28-day age (N/mm²).

Assuming that the planar element confined by beams is represented by a uniaxial model as shown in **Fig. 1**, the following equations are derived according to the equilibrium condition of forces between elements:

$$\begin{aligned} & E_e(t_{i+1/2}, t_j) A \{ \varepsilon(t_{i+1/2}) - \varepsilon_e(t_{i-1/2}) - \varepsilon_f(t_{i+1/2}) \} \\ & + E'_e(t_{i+1/2}, t_j) A' \{ \varepsilon'(t_{i+1/2}) - \varepsilon'_e(t_{i-1/2}) - \varepsilon'_f(t_{i+1/2}) \} \\ & + E''_e(t_{i+1/2}, t_j) A'' \{ \varepsilon''(t_{i+1/2}) - \varepsilon''_e(t_{i-1/2}) - \varepsilon''_f(t_{i+1/2}) \} = 0 \end{aligned} \quad (6)$$

where, A : cross sectional area of the element; $\varepsilon(t_{i+1/2}, t_j)$, $\varepsilon_e(t_{i+1/2}, t_j)$ and $\varepsilon_f(t_{i+1/2}, t_j)$: response strain, restraint strain and free strain, respectively, at Step $t_{i+1/2}$. The superscripts ‘, ‘ and ‘ represent Beams 1 and 2 in **Fig. 1**, respectively. Assuming that the two beams have an equal restraining effect and that the Bernoulli-Euler hypothesis is found true for the strains in the entire sectional areas of the all three elements, the following two equations are derived:

$$\begin{aligned} & E'_e(t_{i+1/2}, t_j) A' \{ \varepsilon'(t_{i+1/2}) - \varepsilon'_e(t_{i-1/2}) - \varepsilon'_f(t_{i+1/2}) \} \\ & = E''_e(t_{i+1/2}, t_j) A'' \{ \varepsilon''(t_{i+1/2}) - \varepsilon''_e(t_{i-1/2}) - \varepsilon''_f(t_{i+1/2}) \} \end{aligned} \quad (7)$$

$$\varepsilon(t_{i+1/2}) = \frac{\{ \varepsilon'(t_{i+1/2}) + \varepsilon''(t_{i+1/2}) \}}{2} \quad (8)$$

According to Equations (3) through (8), the equation for calculating the shrinkage restraint stress σ_{st} of a planar

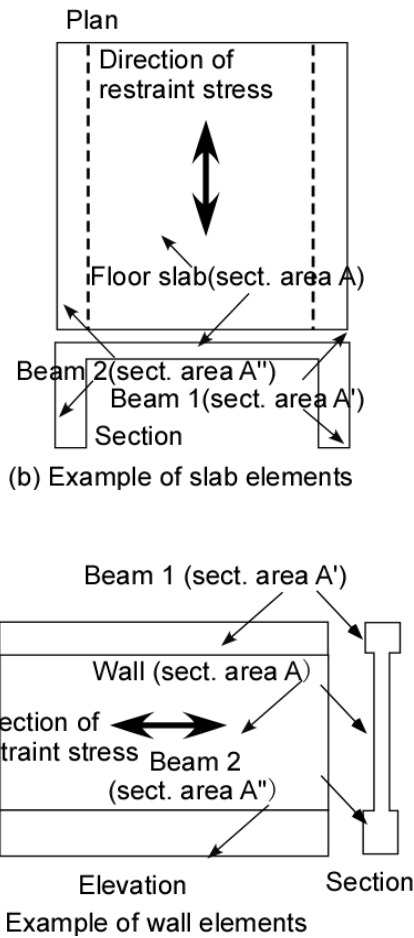


Fig. 1 Uniaxial model of planar elements restrained by beams.

element can be given with explicit functions as follows.

$$\sigma_{st}(t_{j+1/2}) = \sum_{j=1}^i \left[\frac{E_e(t_{j+1/2}, t_j) \{ \Delta \epsilon'_f(t_j) + \Delta \epsilon''_f(t_j) - 2\Delta \epsilon_f(t_j) \} \times \left[\frac{2S'(t_{j+1/2}, t_j) \cdot S''(t_{j+1/2}, t_j)}{S(t_{j+1/2}, t_j) \{ S'(t_{j+1/2}, t_j) + S''(t_{j+1/2}, t_j) \} + 4S''(t_{j+1/2}, t_j) \cdot S''(t_{j+1/2}, t_j)} \right]} \right] \quad (9)$$

where the section stiffness of planar element and two beams, S , S' and S'' , are given by

$$\begin{aligned} S(t_{j+1/2}, t_j) &= E_e(t_{j+1/2}, t_j) A, \text{ and} \\ S'(t_{j+1/2}, t_j) &= E'_e(t_{j+1/2}, t_j) A', \\ S''(t_{j+1/2}, t_j) &= E''_e(t_{j+1/2}, t_j) A'' \end{aligned}$$

The proposed Equation (9) gives shrinkage restraint stress in terms of explicit functions while the stress calculation with the effective Young's modulus method on which Equation (9) is based has been confirmed, by Imamoto (2003), to be satisfactorily accurate in the

analysis of wall elements. Equation (9) is thus expected to have an accuracy level more or less adequate for application to the shrinkage crack control design of actual building elements (Imamoto 2008, Imamoto *et al.* 2004).

3.3 Cracking strength equations

Following the proposal of AIJ (2003a), σ_{cr} is given by the following equation with the reduction coefficient λ , a critical stress-strength ratio, and splitting tensile strength f_t :

$$\sigma_{cr} = f_t \times \lambda \quad (10)$$

A major characteristic of Equations (9) and (10) is that they are expressed in terms of explicit functions, allowing an easy calculation of the dispersion of σ_{cr} and σ_{st} based on the dispersion of variables constituting those functions.

4. Estimation of dispersion

4.1 Estimation equations for dispersion

$COV[S]$ and $COV[R]$ must be known when obtain P_f , using Equation (2), while statistical data regarding actual structures are very few. Hence in this study, $COV[\sigma_{st}]$ and $COV[\sigma_{cr}]$ are calculated based on the dispersion of variables constituting Equations (9) and (10), and the coefficients of variation of S and R are then estimated.

When Y is given by $Y = g(X_1, X_2, X_3, \dots, X_n)$ as a function of several random variables and they are independent from each other, the first term of Taylor series may be taken and the expected value and variance of Y , i.e., $E[Y]$ and $Var[Y]$, are approximated by the following equations (e.g., Ang and Tang 1975), where μ is the expected value of each random variable.

$$E[Y] \approx g(\mu_{X_1}, \mu_{X_2}, \dots, \mu_{X_n}) \quad (11)$$

$$Var[Y] \approx \sum_{i=1}^n C_i^2 Var[X_i] \quad (12)$$

where C_i is the value of partial derivative $\partial g / \partial X_i$ at $\mu_{X_1}, \mu_{X_2}, \dots, \mu_{X_n}$. When the expected value and coefficient of variation of each random variable are known, the expected value and variance of σ_{st} are calculated by applying the Equations (11) and (12) to the Equation (9). In so doing, if $X_i = \phi$, C_i in Equation (12) is given by the following equation. Note that $A' = A''$, $E_e(t_{j+1/2}, t_j) = E'_e(t_{j+1/2}, t_j) = E''_e(t_{j+1/2}, t_j)$ is assumed for simplicity, and

$$C_i = \sum_{j=1}^i \left[\frac{\frac{E[A']}{E[A] + 2E[A']} \times \left[-E[E_c(t_j)]^2 \times \left(E[\Delta \epsilon'(t_j)] + E[\Delta \epsilon''(t_j)] - 2 \times E[\Delta \epsilon(t_j)] \right) \right]}{E[E_{28}] \left(1 + E[\phi(t_{j+1/2}, t_j)] \times E[E_c(t_j)] / E[E_{28}] \right)^2} \right] \quad (13)$$

Likewise, according to Equation (10), σ_{cr} is given by

$$E[\sigma_{cr}] = E[f_t] \times E[\lambda] \quad (14)$$

$$Var[\sigma_{cr}] = E[f_t^2] \times E[\lambda^2] - (E[f_t] \times E[\lambda])^2 \quad (15)$$

4.2 Method of estimating the dispersion of shrinkage restraint stress

In order to estimate the variance of σ_{st} by Equation (12), the expected value and variance of each random variable constituting Equation (9) are needed. To this end, common R/C floor slab elements as schematically shown in **Fig. 1 (b)** are considered and the expected values of the properties of elements are assumed as shown in **Table 1**. The floor slab elements are on a 9-m grid and 300 mm thick, restrained by two footing beams (sectional dimensions: 1500 x 700mm) which are under the ground and assumed free from drying shrinkage. Among the expected values of variables in Equation (9), E_c , ϕ and ε_f require the estimation of their changes with time from the values shown in **Table 1**, for which, the existing literatures are adopted and the details are provided in Appendix. Note that ε_f is given as the drying shrinkage strain in this estimation analysis.

Although there are not enough data available on the dispersion of each random variable, those shown in **Table 2** are estimated on the basis of references. Explained below are the calculation of dispersion, focusing on E_c as an example.

$$\delta = v / \sqrt{2} K_\alpha \quad (16)$$

where, δ : standard deviation; v : maximum deviation; K_α : normal equivalent deviate in accordance with the fraction defective α . Since Kakizaki *et al.* (1977) reported that the difference between the maximum and minimum measured values of E_c for concretes in the same structural elements was approximately 5000 N/mm², this value is assumed as the maximum deviation here. Assuming that E_c follows the normal distribution and the maximum deviation $v_{E_c} = 5000$ N/mm² is equivalent to $\pm K_\alpha \cdot \delta$ of the expected value, δ_{E_c} can be obtained from Equation (16), where $K_\alpha = 1.73$ is assumed corresponding to the fraction defective $\alpha = 4\%$. On the same assumption, among the variables constituting Equation (9), the standard deviations of ϕ as well as A and A' are calculated on the basis of Sato *et al.* (2006) and AIJ (2003b), respectively, and divided by the mean value of each. COV magnitude for ε_f is determined by referring drying shrinkage test data adopting actual Japanese ready-mixed concrete (Momose *et al.* 2007). Summary of these random variables are shown in **Table 2**.

4.3 Method of estimating the dispersion of shrinkage cracking strength

Calculation of the dispersion of σ_{cr} requires the expected values and variance of the two variables constituting Equation (10), which are assumed using the existing literatures. The expected value of f_t , which is one of the variables, is estimated based on the nominal concrete strength given by **Table 1** as shown in appendix 5 in detail.

Table 1 Analytical conditions (Expected values).

Input value	Unit	Value
Dimension of floor slab	mm	9000 x 9000
Thickness of floor slab	mm	300
Section of footing beam	mm	1500 x 700
Nominal concrete strength	N/mm ²	27
Specified concrete strength	N/mm ²	24
Ambient relative humidity	%	60
Ambient temperature	°C	20
Unit water content	kg/m ³	175
Unit mass of concrete	kN/m ³	23
Critical stress-strength ratio	-	0.70

Table 2 Summary of dispersion of random variables.

	Variables	COV	Reference	COV (analysis)
Shrinkage restraint stress	Young's modulus E_c	0.0637	Kakizaki <i>et al.</i> 1977	0.130
	Creep coefficient ϕ	0.173	Sato <i>et al.</i> 2006	
	Free shrinkage strain ε_f	0.0700	Momose <i>et al.</i> 2007	
	Beam section A'	0.0240	AIJ 2003b	
	Floor section A	0.0240	AIJ 2003b	
Shrinkage cracking strength	Splitting strength f_t	0.112	Ueda <i>et al.</i> 1994	0.199
	Reduction coefficient λ	0.166	AIJ 2003a	

The standard deviation of f_t is estimated by Equation (16), assuming the maximum deviation to be 1.02 N/mm² as suggested by Ueda *et al.* (1994). The expected value of λ is set at 0.7 (Makizumi and Ohta 1987), and the maximum deviation at 0.4 (AIJ 2003a).

The dispersions of σ_{st} and σ_{cr} calculated with the proposed methods are not based on direct measured data, and hence, are open to question how accurate the actual conditions are represented. Considering the fact that the dispersion values have been adopted in an arbitrary manner (Nakamura *et al.* 1999), the proposed technique must be of significance to a certain extent in an engineering aspect.

4.4 Results of dispersion estimation

Based on the values shown in **Table 1**, analysis is performed on σ_{st} and σ_{cr} using Equations (9) and (10), respectively. Equation (9) is incremental with respect to material age; the time step is set at one day, and analysis is performed up to a material age of 500th days. Adopted time histories of ε_f , σ_{cr} and ϕ are shown in **Fig. 2 (a)** and **(b)**. The results of analysis on the expected values of σ_{st} and σ_{cr} are found 1.57 and 1.88 N/mm² at 500th day age, respectively.

Next, the results of calculating the coefficient of variation are shown in **Fig. 3**. The values in this figure are obtained by dividing the square root of $C_i^2 Var[X_i]$ in Equa-

tion (12) by the expected value of σ_{st} . Fig. 3 shows the comparison of each variable's contribution on the dispersion of σ_{st} where ε_f is most influential of all random variables. It is also found that the sum of all the impacts of random variables in Equation (12) gives a coefficient of variation of 0.130 as shown in Table 2. From these results, the value of $COV[S]$ applicable to Equation (2) can be set at 0.15 to be slightly conservative.

For σ_{cr} , Equation (15) was performed using the dispersion of random variables given in Table 2. As a result, the coefficient of variation of σ_{cr} was calculated to be 0.199, and the value of $COV[R]$ applicable to Equation (2) was set at 0.2.

5. Calibration by comparison against the cracking of actual structures

5.1 Strategy for determining the safety factor

Among the three set values needed for calculating the cracking probability using Equation (2), this section explains the determination of safety factor γ . It is reasonable to assume that γ takes into account an error created in the process of analytical estimation of S and R with Equations (9) and (10), respectively. Cracking induced by the heat of hydration can be a good example where the safety factor that corresponds to γ here has been set at 1.26 (JSCE 1999), obtained by comparing the results of cracking survey of actual structures (JSCE 1996) against the results of analysis. Likewise in this study, a value of γ is determined by conducting a survey of cracking in actual structural elements and comparing the results against analytical values obtained by Equations (9) and (10).

5.2 Analytical cases and quantification of crack-ing conditions

As shown in Fig. 4, four analytical cases are selected: two cases of wall elements restrained by upper and lower beams (hereinafter called "W-1" and "W-2", respectively), and two cases of floor elements restrained by steel beams in actual structural frames ("S-1" and "S-2"). The former two are the model structural frames in experiments, whose cracking data can be given by an existing literature (Imamoto 2003). The latter two have been sampled from continuously-spanned floor slab elements of actual structures. One grid is selected for modeling and subjected to shrinkage restraint stress analysis in the longitudinal direction. These elements are subjected to a survey on the width and length of the cracks developed for at least one incremental material age, allowing a comparison against the analytical results.

The cracking survey of S-1 was performed with a 4-story steel-structured office building, and the entire R/C slab floors with steel deck plates on the 2nd, 3rd and 4th floors were surveyed. The number of spans was 7 and 3 in the longitudinal and transverse directions, respectively. The survey S-2 was performed with a 4-story distribution facility constructed with a combined structural system having R/C columns and steel beams. The survey was

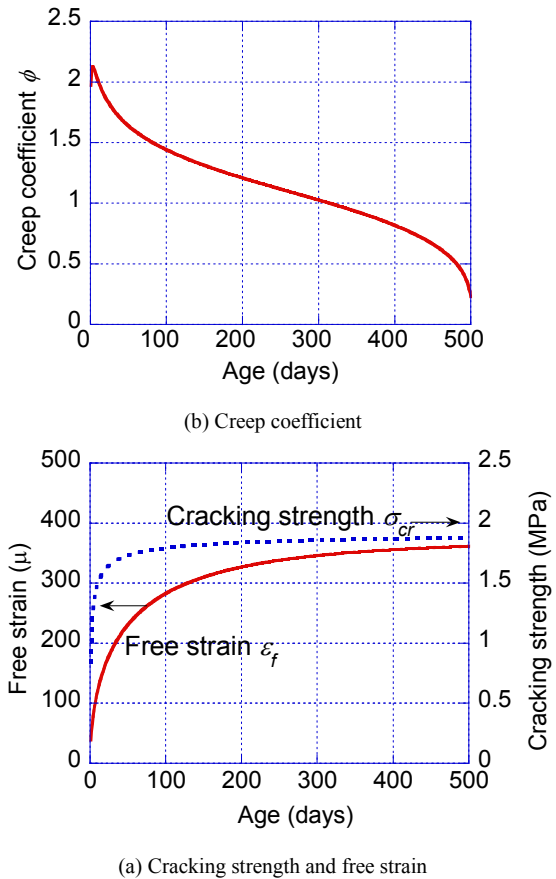


Fig. 2 Time dependent changes in variables.

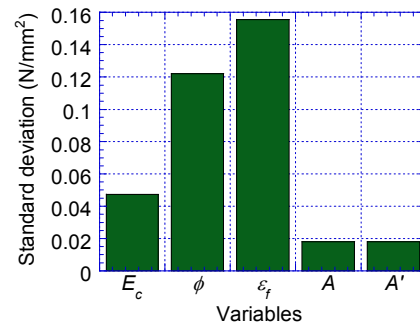


Fig. 3 Calculation results of variables' contribution to shrinkage restraint stress dispersion.

performed for the 4th floor which was constructed with steel deck plates. The number of spans was 10 and 5 in the longitudinal and transverse directions, respectively, but 6 x 5 continuous spans were selectively surveyed. The crack width is represented by the maximum width of a single crack.

For the purpose of quantifying the cracking condition of each element here, a value obtained by dividing the product of crack width and crack length by floor area is defined as the crack density used for comparison against

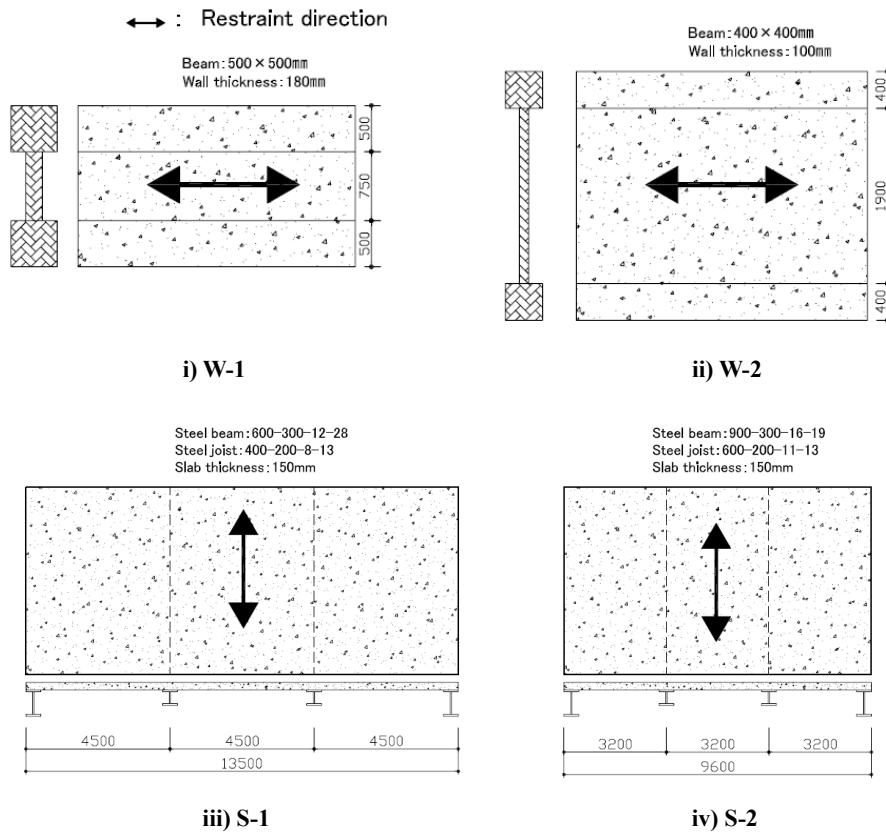


Fig. 4 Structural elements selected as analytical target.

the analytical results. The crack density of each analytical case and the measured concrete age are shown in **Table 3**.

5.3 Method of analysis

Equation (9) that calculates shrinkage restraint stress was subjected to further improvement for analytical accuracy. For simplicity, it did not take into account the influence of reinforcing bars inside the beam and planar elements. Therefore, to reflect this influence, each element is assumed as a uniaxially constraint specimen internally restrained by reinforcing bars, and a preliminary stress analysis was performed with Equation (17), which is derived from Equation (9). Using σ_{st}^i , i.e. the results of the preliminary stress analysis, shrinkage strain ϵ_f^i induced by internal restraint was calculated by Equation (18), while σ_{st} is calculated by Equation (9) assuming $\epsilon_f = \epsilon_f^i$. Finally, as shown in Equation (19), the stress value σ_{st}^i derived from Equation (17) is added to σ_{st} , which is induced by external restrained and obtained in Equation (9), and the sum worked out to be the total shrinkage restraint stress σ_{st}^w .

$$\sigma_{st}^i(t_i) = \sum_{j=1}^i E_e(t_i, t_j) \frac{0.5(A_s E_s)^2}{A_c E_e(t_{j+1/2}, t_j) (A_s E_s) + (A_s E_s)^2} \{-2\Delta\epsilon_f(t_j)\} \tag{17}$$

Table 3 Result of crack survey.

Case	Inspection	Age (day)	Crack density (mm ² /m ²)
W-1	Just before cracking	34	-
	Crack observation	35	6.3
	Crack observation	65	13.0
W-2	Just before cracking	36	-
	Crack observation	62	38.9
		84	63.2
		209	63.0
S-1	Crack observation	124	42.6
		133	29.5
		137	48.7
S-2	Crack observation	136	147.0

Floor types of S-1 are the same from 2nd and 4th floor where inspection was performed throughout.

$$\epsilon_f^i(t_i) = \left\{ \sigma_{st}^i(t_i) \cdot A_c \right\} / (A_s \cdot E_s) \tag{18}$$

$$\sigma_{st}^w(t_i) = \sigma_{st}(t_i) + \sigma_{st}^i(t_i) \tag{19}$$

where, A_s : sectional area of reinforcing bars (mm²); A_c : sectional area of concrete (mm²); E_s : Young's modulus of reinforcing bar (N/mm²).

Table 4 shows the input items for each element in **Fig. 4**.

Table 4 List of input values for the structural elements subjected to analysis.

	Member	Details	Analysis				Original design of case study
			W-1	W-2	S-1	S-2	
Type of structure	Planer	Width x Thickness (mm)	750 x 180	1900 x 100	13500 x 150	9600 x 150	9000 x 180
		Reinforcing bar (ratio)	D13@125 (0.56 %)	D10@100 (0.68 %)	D13@200 w Deck t=1 mm (1.5 %)	D13@150 D13@200 Deck t=1mm(1.7 %)	D13@150 D10@150 Lattice f6@150 Deck t=1mm(1.4 %)
	Beam 1	Section (mm)	500 x 500	400 x 400	H-600-300-12-28 H-400-200-8-13	H-900-300-16-19 H-600-200-11-13	H-800-300-14-26 H-588-300-12-20
		Reinforcing bar	D22-6	D19-8	-	-	-
	Beam 2	Section (mm)	500 x 500	400 x 400	H-600-300-12-28 H-400-200-8-13	H-900-300-16-19 H-600-200-11-13	H-800-300-14-26
		Reinforcing bar	D22-6	D19-8	-	-	-
Material property	Planer or Beam 2	28-day compressive strength (N/mm ²)	31.8	32.9	36.0	37.2	27.0
		28-day Young's modulus (N/mm ²)	25100	24175	-	32600	-
		Water/binder ratio (%)	50	50	48.6	51	55
		Unit water (kg/m ³)	180	180	162	175	170
		Cement type	OPC	OPC	OPC	OPC	OPC
	Beam 1	28-day compressive strength (N/mm ²)	30.6	31.5	-	-	-
		28-day Young's modulus (N/mm ²)	22400	23400			
		Water/binder ratio (%)	50	50			
		Unit water (kg/m ³)	180	180			
		Cement type	OPC	OPC			
Others	-	Demolding	3-day	8-day	-	-	-
		Placement ages	Beam1 placed at 7-day after Beam 2	Beam1 placed at 30-day after Beam 2	-	-	-
		R.H. (%)	60	60	60	60	60

The Young's modulus of steels E_s is assumed as 210000 N/mm² without exception. With regard to the two cases of floor elements in Fig. 4, the floor slab is restrained by two girders (beams) and two joists, and the sum of the sectional area of a girder and a joist is assumed to be the sectional areas of *Beams 1* and *2*, respectively, while E_c , ϕ , ε_f and f_t were calculated with the method explained in Appendix.

5.4 Results of the analysis

Figure 5 shows changes with time of the calculated shrinkage strain of each analytical case up to a material age of 200 days. The origin of the material age was the point when concrete was placed for the planar element. For wall elements in Fig. 5 (a) and (b), the difference in the shrinkage strain of beam concrete and that of wall concrete is the major driving force of shrinkage restraint stress, while this shrinkage strain difference of *W-1*(a) is approximately 200 μ and *W-2*(b) shows a bigger value of 400 μ . This may be attributed to a larger wall thickness of *W-1* than that of *W-2*. For floor elements shown in Fig. 5 (c) and (d), the external restraint body such as steel beams do not undergo shrinkage and the shrinkage strain of floor concrete serves as the major driving force of the shrinkage restraint stress. In these figures, ε_f^i that takes into account the internal restraint shows a smaller absolute strain than ε_f ,

reflecting the influence of internal restraint.

Relationship between shrinkage restraint stress and cracking strength of each analytical case is shown in Fig. 6. The results up to a material age of 200 days show that the total shrinkage restraint stress σ_{st}^w exceeds σ_{cr} in Fig. 6 (a), (b) and (d) and σ_{st}^w is approaching σ_{cr} in Fig. 6 (c). For wall elements in Fig. 6 (a) and (b), σ_{st}^w accounts for as little as approximately 20% of σ_{st}^w at maximum, while for floor elements in Fig. 6 (c) and (d), the percentage becomes larger, i.e., 30 to 50%, indicating that internal restraint is more significant. One reason is that, in the two analytical cases for floor elements, deck plates are treated as reinforcing bars hence the area of reinforcement becomes twice as large as that of wall elements, resulting in an increase in the shrinkage restraint stress. Another reason is that the level of restraint by the beams is relatively smaller in floor elements than that in wall elements, hence the shrinkage restraint stress by external restraint tends to be smaller in floor elements. Thus, one may conclude that the higher the volume of reinforcing bars and the smaller the external restraint, the bigger the error created by the ignorance of internal restraint impacts. It is shown that the method taking into account the internal restraint allows the calculation of shrinkage restraint stress induced in planar elements based on the cracking mechanism that represents

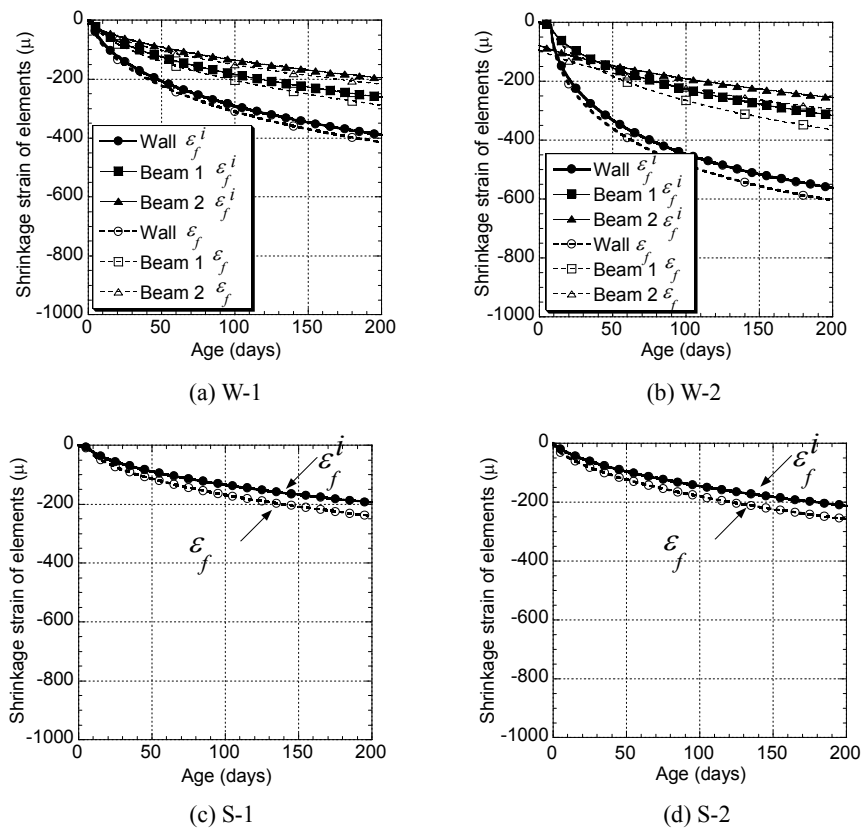


Fig. 5 Shrinkage strain of each element.

the actual phenomena more realistically, thereby being able to enhance the accuracy of stress estimation. In the following discussions, σ_{st}^w is used as the shrinkage restraint stress instead of σ_{st} , and $\eta^w (= \sigma_{st}^w / \sigma_{cr})$ as the stress-strength ratio instead of η .

5.5 Discussions and determination of safety factor

Analysis results on η^w with time of each element are shown in Fig. 7 where the two cases of wall elements show a larger η^w than the two cases of floor elements. This may be attributed to the fact that the stiffness of restraining beam elements is relatively smaller in the floor elements.

Relationship between η^w and the crack density obtained in the crack survey is shown in Fig. 8, where a correlation is found between η^w and the crack density and thus the control of η^w may lead to restriction of cracking to a minor level even if developed. Since the influence of η^w on the crack density is different between wall and floor slab elements, linear approximation is separately shown for these two types of elements respectively in the figure. It is clearly exhibited that, with the same stress-strength ratio, the floor slab elements undergo notably extensive cracking. Major reasons for this appear that: 1) the analysis does not consider the impacts of the fact that, during placing, a floor slab is susceptible to micro cracking caused by deformation and vibration due to the lower stiffness of the deck

plates, and 2) beam ends are prone to cracking because the flexural moment induced by loading during construction process is applied to the floor slab element.

In order to reduce shrinkage cracks, it is generally accepted to decrease the restraint strain due to the drying shrinkage and the degree of restraint. Since the restraint strain comprises creep strain and elastic strain directly linked to σ_{st} , reduction of the restraint strain can lower the value of σ_{st} and consequently that of η^w . On the other hand, crack density is defined as the product of the number and width of cracks when assuming a uniaxial element having a unit area. It has been proven, by for example Hashida (2005), or Nejadi and Gilbert (2004), that the smaller the restraint strain, the smaller the width and number of cracks become. Thus, a positive correlation between η^w and crack density may be expected through the influence of restraint strain as shown in Fig. 8. Nonetheless, it should be one of the future tasks to examine in detail how structural, material and environmental factors affect this correlation.

Next, an example of the determination of the safety factor using Fig. 8 is discussed. According to the figure, it is assumed that hardly any cracking occurs if a value of η^w is smaller than the intersection of the X-axis with each approximated line of wall and floor slab elements. Because η^w shows a value of approximately 0.6 at the intersection for both wall and floor elements, the critical stress-strength ratio for cracking is assumed to be $\eta^w = 0.6$. With an as-

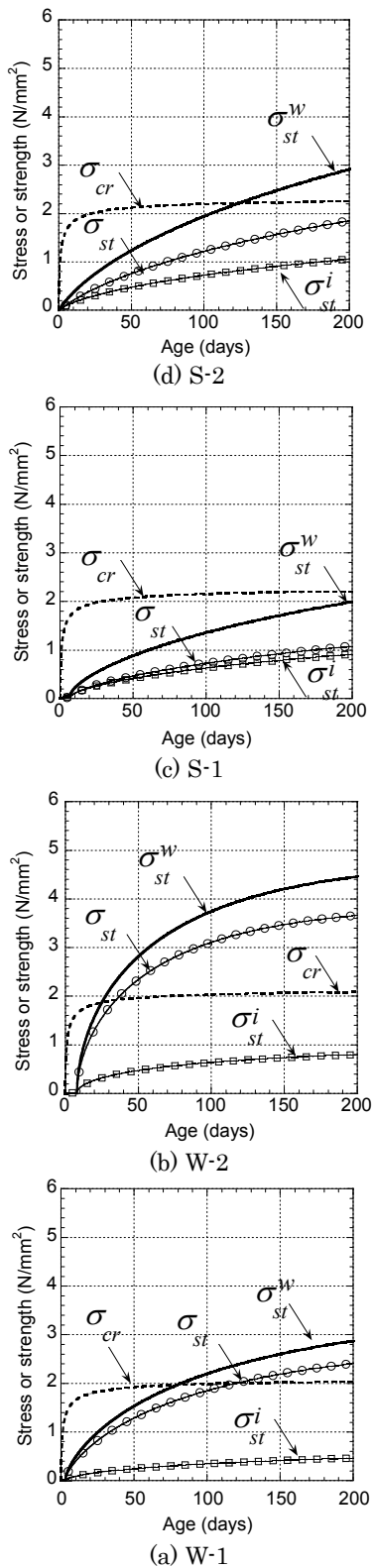


Fig. 6 Total shrinkage restraint stress and cracking strength of planar members.

sumption that the cracking probability at this critical point is equivalent to an acceptable engineering defective frac-

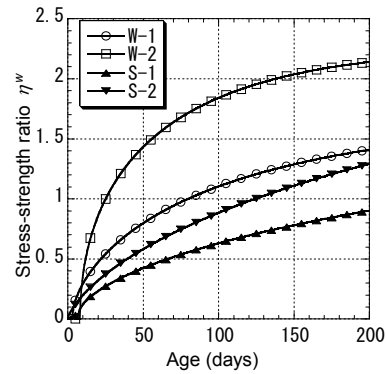


Fig. 7 Analytical results for changes with time in the stress-strength ratio

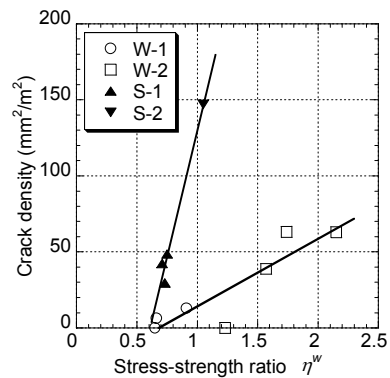


Fig. 8 Impacts of stress-strength ratio on cracking density.

tion such as P_{fa} , the following equation is derived from Equation (2):

$$P_{fa} = \Phi \left[\frac{(\xi-1)}{\sqrt{COV[R]^2 + \xi^2 \cdot COV[S]^2}} \right] \quad (20)$$

Adopting the same acceptable defective fraction $P_{fa} = 0.04$ as reference (AIJ 2003b), which is applied when determining the specified compressive strength with respect to the assumed compressive strength in mix proportion design of concrete, and substituting 0.2 for $COV[R]$, 0.15 for $COV[S]$ and $\eta = \eta^w = 0.6$ in solving Equation (20), we obtain $\gamma \approx 1.05$.

The result of this trial calculation, $\gamma \approx 1.05$, should serve as a useful reference in the determination of safety factor, while the data in Fig. 8 used for the calculation are limited, and the guarantee as an adequate level of engineering safety still remains as a concern. Thus, to be conservative in the calculation of cracking probability, an increased value of 1.5, instead of 1.05, is adopted for γ tentatively. The shrinkage crack risk curve obtained by adopting $\gamma = 1.5$, $COV[S] = 0.15$ and $COV[R] = 0.2$ is shown in Fig. 9 where the cracking probability is restricted to 0.04, a level at which hardly any cracking occurs, with a stress-strength ratio of approximately 0.4. Relationship between crack density and cracking probability for the four analytical

cases derived from the shrinkage crack risk curve is shown in Fig. 10 where it is confirmed, within the scope of this study, that controlling the cracking probability to $P_{fa} = 0.04$ or a lower level can serve as the considerably conservative assessment of both wall and floor elements against an actual cracking level. Upon accumulation of sample data in the future, the safety factor determined here may be reduced from 1.5, providing that the engineering safety is not sacrificed.

It should be noted that for floor slabs, the impacts of vertical load should be considered in the calculation of η^w and P_f . The slabs studied here are constructed with deck plates as permanent form works, which do not require supports upon construction process, and their deadweight is assumed negligible as is sustained by the deck plates. Furthermore, the cracking survey was performed before the completion of buildings when no live loads had been applied, hence the vertical load was limited to the loading during construction work and thus its impacts are limited. On the other hand, ordinary R/C slabs that use supports during construction are subjected to a significant level of flexural stress by deadweight loading after removing supports, when the flexural stress is added to σ_{st} and its impacts should properly be considered.

6. Application examples of the proposed control technique

6.1 Outline of the applied structure and the analysis of originally designed elements

The structural elements chosen for the application are floor slabs with truss bars and deck plates constructed on the 2nd floor of a 2-story steel-structured distribution facility (See Fig. 11 for the floor plan). Details and modeling of the elements are shown in Fig. 12. The specifications of bar arrangements in the original design and concrete properties are shown in Table 4.

The results of analysis performed on σ_{st}^w and σ_{cr} of the originally designed elements according to the procedures described in Section 5.3 and the estimated P_f using the shrinkage crack risk curve of Fig. 9 are shown in Fig. 13 and Fig. 14, respectively. As a result, cracking was found inevitable, because the shrinkage restraint stress of originally designed elements exceeded the cracking strength at a material age of 300 days onwards in Fig. 13, and the maximum value of P_f becomes nearly 1.0 in Fig. 14.

6.2 Analytical results of improved design and comparison in terms of the cracking condition

Various techniques have been proposed to reduce cracking risk, while the ‘‘Crack-Reducing Concrete’’ (CRC), using a high-performance expansive agent and a shrinkage-reducing agent (Momose *et al.* 2005) was adopted in this study. Although no method of calculating P_f had been established for CRC, this study attempted to perform quantitative evaluation of crack-reducing effects by simply considering the expanding and shrinking characteristics of CRC.

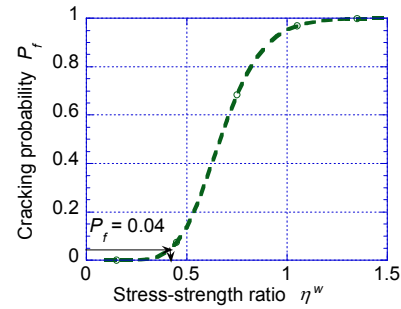


Fig. 9 Proposed shrinkage crack risk curve.

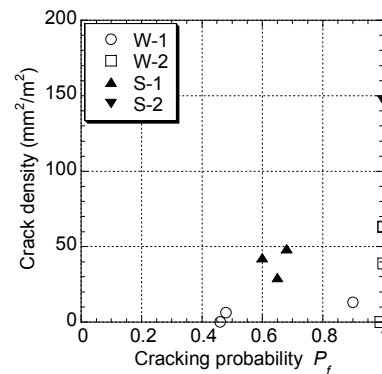


Fig. 10 Influence of cracking probability on crack density.

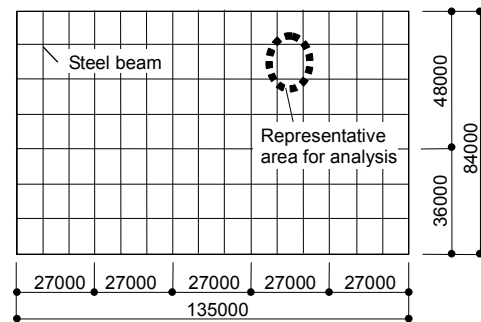


Fig. 11 Floor plan of the building to which the proposed crack control method was applied (Unit: mm).

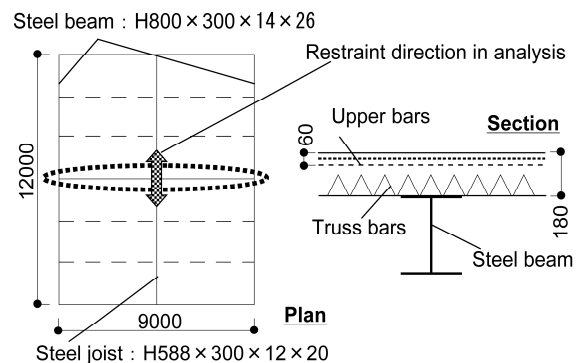


Fig. 12 Configuration of the floor slab subjected to the crack control analysis (Unit: mm).

The crack-reducing effects of CRC are broadly categorized into the chemical pre-stressing through expansion effects of an expansive additive and a reduction of long-term drying shrinkage by a shrinkage reducing agent. The evaluation was achieved in a simplified manner by adopting a compressive stress of 0.8 N/mm^2 as the initial value of chemical pre-stressing of the actual structure referring to the laboratory restraint tests. Likewise, for the reduction of long-term drying shrinkage, the drying shrinkage strain of CRC was reduced to three quarter of that of ordinary concrete on the basis of the laboratory drying shrinkage tests. The changes with time in σ_{st}^w and P_f for CRC application are compared against those of the original design in Fig. 13 and Fig. 14, respectively, where use of CRC was found to bring about significant improvements, showing the possibility of substantial reduction of the cracking risk; the shrinkage restraint stress is significantly reduced, as illustrated by the reduction of P_f to approximately 0.2 from a value of approximately 1.0 in the case of ordinary concrete. Thanks to the results, CRC was actually applied to the construction stage.

At the time of completion of construction, 3 to 4 months after the placing of CRC, few cracks were observed on the floor slabs. The shrinkage restraint stress of concrete, calculated on the basis of concrete strain measured directly above the steel beam of the actual frame (Kanda *et al.* 2004), decreased gradually after reaching the maximum compressive stress of 0.75 N/mm^2 at an early age. Then on the 80th day, there was a remaining level of 0.3 N/mm^2 on the compressive side (Kanda *et al.* 2005), showing more or less good agreement with the results shown in Fig. 13. From these results, the redesign was reasonable on the whole, and it is confirmed that the value of σ_{st}^w calculated by the proposed technique was not far from the actual value. Thus, the control technique proposed in this study has been proven effective in an actual construction project, with its accuracy acceptable to a certain extent.

7. Conclusions

Focusing on planar elements restrained with beams, this study has proposed a shrinkage crack control technique capable of assessing the shrinkage cracking risk in terms of cracking probability P_f , verified its accuracy and confirmed its effectiveness through application to an actual construction project. The major findings of this study are summarized as follows.

- 1) The explicit functions were derived and expressed in terms of Taylor series for the driving force of shrinkage crack, i.e., shrinkage restraint stress, and for the resisting force, i.e., cracking strength. They are used for calculating the dispersion, and consequently, application of a coefficient of variation of approximately 0.15 and 0.2, respectively was found feasible.
- 2) Comparative estimation of the analytical results of stress-strength ratio (ratio of shrinkage restraint stress to the cracking strength) and the results of crack survey on actual structural elements allowed the safety

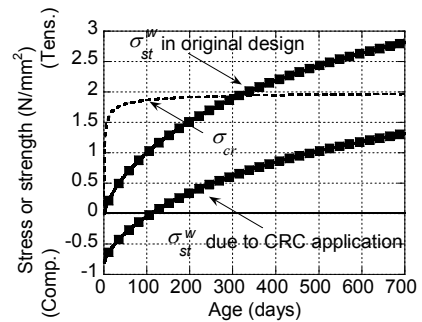


Fig. 13 Analytical results of stress and strength.

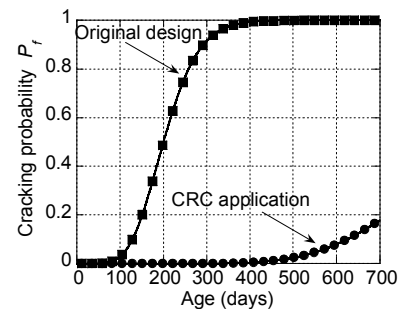


Fig. 14 Calculation results of cracking probability.

factor of 1.5 for the conservative calculation of P_f .

- 3) Correlation between the stress-strength ratio and extent of cracking indicated a possibility of controlling cracking to a minor level by reducing the stress-strength ratio.
- 4) When taking account not only of the external restraint by beams but also of the internal restraint by reinforcing steels, the calculation of shrinkage restraint stress may contribute to an improvement of accuracy.
- 5) The proposed crack control technique was applied to an actual construction project and its effectiveness was consequently confirmed proposing relevant solutions. Though limited, the accuracy of the technique was verified to a certain extent.

Because the crack control technique proposed in this study does not consider such factors as an increase in the degree of restraint in continuous spans, impacts of thermal strain and vertical load on floor slab elements, its application has limitations where these factors have major impacts. If the proposed technique is enhanced to involve these factors, an improved accuracy and application to more general and a wider scope of projects will become possible. Incorporation of these factors and detailed studies of the accuracy are left as the subjects of the future research.

References

- AIJ, (2002). "Recommendation for Practice of Crack Control in Reinforced Concrete Buildings-Design and

- Construction.” Japan Architectural Institute. (in Japanese)
- AIJ, (2003a). “Shrinkage Cracking in Reinforced Concrete Structures – Mechanisms and Practice of Crack Control.” Japan Architectural Institute. (in Japanese)
- AIJ, (2003b). “Japanese Architectural Standard Specification, JASS 5 Reinforced Concrete Work.” Japan Architectural Institute. (in Japanese)
- Ang, A. and Tang, H. T. (1975). “Probability Concepts in Engineering Planning and Design, Basic Principles.” New York: John Wiley & Sons.
- Ang, A. and Tang, H. T. (1984). “Probability Concepts in Engineering Planning, Decision, Risk, and Reliability.” New York: John Wiley & Sons.
- Bolander, J. E. and Berton, S. (2004). “Simulation of shrinkage induced cracking in cement composite overlays.” *Cement and Concrete Composites*, 26, 7, 861-871.
- fib (1990). “CEB-FIP model code 1990.” *fédération internationale du béton*, 2.
- Hashida, H. (2005). “A Prediction of Shrinkage Cracking for External RC Wall.” *Summaries of Technical Papers of Annual Meeting*, AIJ, A-1, 645-646. (in Japanese)
- Imamoto, K. (2003). “A simplified calculation method for shrinkage induced stresses of various kinds of concrete walls.” *Proceedings of the Japan Concrete Institute*, 25, 1, 413-418. (in Japanese)
- Imamoto, K. (2008). “Simplified prediction of drying shrinkage stress in reinforced concrete building walls.” *Journal of Advanced Concrete Technology*, 6(1), 111-120.
- Imamoto, K., Kanda, T., Momose, H. and Mihashi, H. (2004). “Performance design of shrinkage cracking control – Part 1, 2, and 3.” *Proceeding of the 75th Architectural Research Meetings*, Kanto Chapter, Architectural Institute of Japan, 75-I, 41-52. (in Japanese)
- Iwaki, R., Natsume, T., Murayama, Y., Murata, T. and Onuki, H. (1980). “Analytical method for thermal stress evaluation induced by heat of hydration.” *Kajima Technical Research Institute Report*, 28, 45-52. (in Japanese)
- JCI, (2001). “Committee Report and Symposium proceedings on Time-dependent Deformation of Concrete Structures due to Shrinkage and Creep.” Japan Concrete Institute, JCI-C52, 164-165. (in Japanese)
- JSCE, (1996). “State of the Art of Current Mass Concrete Technology.” Concrete Engineering Series, 14. (in Japanese)
- JSCE, (1999). “Complementary for Standard Specifications for Concrete Structures.” Concrete Library, 99. (in Japanese)
- JSCE, (2002a). “Standard Specifications for Concrete Structures 2002, Materials and Construction.” Guidelines for Concrete No.6.
- JSCE, (2002b). “Standard Specifications for Concrete Structures 2002, Structural Performance Verification.” Guidelines for Concrete No.3.
- Kakizaki, M., Sato, H., Nakanishi, M. and Nara, Y. (1977). “Field study for testing method of concrete elastic modulus (Part 5 Elastic modulus and compressive strength of concrete in full scale elements).” *Summaries of Technical Papers of Annual Meeting*, 121-122. (in Japanese)
- Kanda, T., Momose, H. and Sakuramoto, F. (2004). “Experimental investigation of anti-cracking effects in concrete Slab applying expansive agent and shrinkage reducing agent.” *JCI Annual Conference Proceedings*, 26, 1, 501-506. (in Japanese)
- Kanda, T., Momose, H., Yasuzawa, T. and Furukawa, H. (2005). “Anti-cracking approach for RC structures using crack reducing concrete (part 1 and 2).” *Summaries of Technical Papers of Annual Meeting*, AIJ, A-1, 651-654. (in Japanese)
- Kwak, H. G. and Ha, S. J. (2006). “Non-structural cracking in RC walls: Part II. Quantitative prediction model.” *Cement and Concrete Research*, 36, 761-775.
- Li, L., Berke, N. S., Durning, T. A. and Bentur, A. (2006). “Computer modeling of bridge deck cracking at early ages.” *RILEM Proceedings pro051: Advances in Concrete through Science and Engineering*.
- Makizumi, T. and Ohta, T. (1987). “Shrinkage cracking of concrete subject to the external uniaxial restraint.” *Journal of Materials, Concrete Structures and Pavements*, JSCE, 378/V-6, 137-146. (in Japanese)
- Momose, H., Kanda, T. and Sakuramoto, F. (2004). “Expansion and shrinkage properties of concrete using low heat portland cement and expansive admixture.” *JCI Annual Conference Proceedings*, 26, 1, 495-500. (in Japanese)
- Momose, H., Kanda, T., Ishida, M. and Sakuramoto, F. (2005). “A study on resistance against cracking of concrete using expansive admixture and shrinkage reducing admixture.” *Journal of Structural and Construction Engineering*, 587, 7-14. (in Japanese)
- Momose, H., Kanda, T., Imamoto, K. and Mihashi, H. (2007). “Comprehensive field study for drying shrinkage of Japanese ready-mixed concrete (Part 1).” *Summaries of Technical Papers of Annual Meeting, Materials and Construction*. (in Japanese)
- Nakamura, H., Hamada, S., Tanimoto, T. and Miyamoto, A. (1999). “Study on the estimation of thermal cracking for the mass concrete structures having uncertain properties.” *ACI Structural Journal*, 96, 4, 509-518.
- Nejadi, S. and Gilbert, I. (2004). “Shrinkage cracking and crack control in restrained reinforced concrete members.” *ACI Structural Journal*, 101, 6, 840-845.
- Noguchi, T. and Tomosawa, F. (1995). “Relationship between compressive strength and various mechanical properties of high strength concretes.” *Journal of Structural and Construction Engineering*, 472, 11-16. (in Japanese)
- Rüsch, H. and Jungwirth, D. (1976). “*Stahlbeton – Spannbeton Band 2*.” Werner-Verlag GmbH.
- Sato, Y., Kiyohara, C., Imamoto, K., Teranishi, K., Mihashi, H. and Hamanaga, Y. (2006). “Study on the prediction formula for time-dependent strain of

concrete.” *Journal of Structural and Construction Engineering*, AIJ, 599, 9-15. (in Japanese)

Tazawa, E. and Miyazawa, S. (1997). “Estimation of autogenous shrinkage of concrete.” *Journal of Materials, Concrete Structures and Pavements*, JSCE, 571/V-36, 211-219. (in Japanese)

Tokumaru, H., Shibata, H., Okamura, H., Hasegawa, T., Soeda, T., Nakamizo, T., Akitsuki, K. and Yamakawa, S. (1987). “*Handbook of Statistical Engineering*.” Chapter 12, 547-552. (in Japanese)

Ueda, M., Sato, M., Hasebe, N. and Okuda, H. (1994). “Study on size effect of concrete – direct tensile strength.” *Proceedings of the Japan Concrete Institute*, 16, 2, 69-74. (in Japanese)

van Breugel, K. and Lockhorst, S. J. (2001). “Stress-based crack criterion as a basis for prevention of through-cracks in concrete structures at early ages.” *RILEM Proceedings PRO 23: Early Age Cracking in Cementitious Systems EAC'01*, 229-236.

Appendix

a) Compressive strength (fib 1990)

$$f_{cm}(t) = b_{cc}(t) \cdot f_{cm}(28) \quad (\text{appendix 1})$$

$$b_{cc}(t) = \exp(s \cdot (1 - (28/t)^{0.5})) \quad (\text{appendix 2})$$

where $f_{cm}(t)$: compressive strength at an age of t (N/mm²)

s : cement factor (=0.25)

b) Young's modulus (AIJ 2003b; fib 1990)

$$E_c(t) = b_E(t) \cdot E_c(28) \quad (\text{appendix 3})$$

$$E_c(28) = 33500 \cdot k_1 \cdot k_2 \times (r/2.4)^{2.0} \cdot (F_c/60)^{1/3} \quad (\text{appendix 4})$$

where $E_c(t)$: Young's modulus at an age of t (N/mm²)

$b_E(t)$: rate factor (=bcc(t)0.5)

k_1, k_2 : coefficients (1.0)

r : specific mass (ton/m³)

F_c : design strength (N/mm²)

c) Tensile strength (Noguchi and Tomosawa 1995)

$$f_t(t) = 0.291 \cdot f_{cm}(t)^{0.637} \quad (\text{appendix 5})$$

where $f_t(t)$: tensile strength at an age of t (N/mm²)

d) Creep coefficient (fib 1990)

$$\phi(t, t_0) = \phi_c \cdot \beta_c(t, t_0) \quad (\text{appendix 6})$$

$$\phi_c = \phi_{RH} \cdot \beta(f_{cm}(28)) \cdot \beta(t_0) \quad (\text{appendix 7})$$

$$\phi_{RH} = 1 + (1 - RH/100) / (0.46 \cdot (h/100)^{1/3}) \quad (\text{appendix 8})$$

$$\beta(f_{cm}(28)) = 5.3 / ((f_{cm}(28)/10)^{0.5}) \quad (\text{appendix 9})$$

$$\beta(t_0) = 1 / (0.1 + (t_{0(cem)}/1)^{0.2}) \quad (\text{appendix 10})$$

$$t_{0(cem)} = t_0 \cdot ((9 / (2 + (t_0/1)^{0.5})) + 1)^{\alpha} > 0.5 \quad (\text{appendix 11})$$

$$h = 2 \times A_c / u \quad (\text{appendix 12})$$

$$\beta_c(t, t_0) = (((t - t_0)/1) / (\beta_{RH} + (t - t_0)/1))^{0.3} \quad (\text{appendix 13})$$

$$\beta_{RH} = 150 \cdot (1 + (1.2 \times RH/100)^{18}) \cdot h / 100 + 250 \leq 1500$$

(appendix 14)

where (t,t₀): creep coefficient at an age of t when specimen loaded at t_0

α : cement factor (= 0)

RH : relative humidity (%), h : effective thickness (mm)

e) Drying shrinkage (Momose *et al.* 2004; JSCE 2002b; Rüsich and Jungwirth 1976)

$$\varepsilon'_{cs}(t, t_{0sh}) = k_s(t, t_{0sh}) \cdot \varepsilon'_{sh} \quad (\text{appendix 15})$$

$$\varepsilon'_{sh} = 500 - 780 \cdot (1 - \exp(RH/100)) - 380 \cdot \log_e W + 50 \cdot$$

$$(\log_e(25)/10)^2 \quad (\text{appendix 16})$$

$$k_s(t, t_{0sh}) = k_a \cdot (1 - \exp(-k_b \cdot (t - t_{0sh})^{kc})) \quad (\text{appendix 17})$$

$$k_a = 0.5765 \cdot \exp(-0.0104 \cdot V/S) + 0.7137 \quad (\text{appendix 18})$$

(1.19 when $V/S \leq 25$ and 0.70 when $V/S \geq 800$)

$$k_b = 0.5431 \cdot \exp(-0.3346 \cdot V/S^{0.4608}) \quad (\text{appendix 19})$$

(0.1249 when $V/S \leq 25$ and 0.0004 when $V/S \geq 800$)

$$k_c = -0.7140 \cdot \exp(-0.0011 \cdot V/S) + 1.2361 \quad (\text{appendix 20})$$

(0.53 when $V/S \leq 25$ and 0.94 when $V/S \geq 800$)

where $\varepsilon'_{cs}(t, t_{0sh})$: shrinkage strain at an age of t (μ)

W : unit water (kg/m³), V : volume (mm³)

S : outdoor exposing area (mm²), t_{0sh} : age when drying starts (day)

f) Autogenous shrinkage (Tazawa and Miyazawa 1997)

$$\varepsilon_c(t) = \varepsilon_c \cdot \varepsilon_{c0}(W/B) \times \beta(t) \quad (\text{appendix 21})$$

when $0.2 \leq W/B \leq 0.5$

$$\varepsilon_{c0}(W/B) = 3070 \cdot \exp(-7.2(W/B)) \quad (\text{appendix 22})$$

when $W/B > 0.5$

$$\varepsilon_{c0}(W/B) = 80 \quad (\text{appendix 23})$$

$$\beta(t) = 1 - \exp(-a(t - t_0)^b) \quad (\text{appendix 24})$$

where $\varepsilon_c(t)$: autogenous shrinkage strain at an age t (μ)

γ_c : factor representing the effects of cement and admixture

a : constant (0.1 for case S-2 and 0.03 for other cases)

b : constant (0.7 for case S-2 and 0.8 for other cases)